AD/A-004 001

EFFECTS OF CLUSTER POROSITY ON THE TENSILE PROPERTIES OF BUTT-WELDMENTS IN T-1 STEEL

E. M. Honig, Jr.

Army Construction Engineering Research Laboratory
Champaign, Illinois

November 1974

REPORT DOCUMENTATION PAGE		READ INSTRUCTIONS BEFORE COMPLETING FORM
1. REPORT NUMBER TECHNICAL REPORT M-109	2. GOVT ACCESSION NO.	3. RECIPIENT'S CATALOG NUMBER AD/A-004001
4. TITLE (and Subtitle) EFFECTS OF CLUSTER POROSITY ON THE TENSILE PROPERTIES OF BUTT-WELDMENTS IN T-1 STEEL		5. TYPE OF REPORT & PERIOD COVERED
		6. PERFORMING ORG. REPORT NUMBER
7. AUTHOR(s) E. M. Honig, Jr.		8. CONTRACT OR GRANT NUMBER(s)
9. PERFORMING ORGANIZATION NAME AND ADDRESS CONSTRUCTION ENGINEERING RESEARCH LABORATORY P.O. Box 4005 Champaign, Illinois 61820		10. PROGRAM ELEMENT, PROJECT, TASK AREA & WORK UNIT NUMBERS OK1-02-102
11. CONTROLLING OFFICE NAME AND ADDRESS		12. REPORT DATE November 1974
		13. NUMBER OF PAGES 32
14. MONITORING AGENCY NAME & ADDRESS(if different from Controlling Office)		15. SECURITY CLASS. (of this report) UNCLASSIFIED
		15a. DECLASSIFICATION/DOWNGRADING SCHEDULE

16. DISTRIBUTION STATEMENT (of this Report)

Approved for public release; distribution unlimited

17. DISTRIBUTION STATEMENT (of the abstract entered in Block 20, if different from Report)

18. SUPPLEMENTARY NOTES

19. KEY WORDS (Continue on reverse side if necessary and identify by block number)

cluster porosity
tensile properties
butt-weldments

PRICES SUBJECT TO CHANGE

20. ABSTRACT (Continue on reverse side if necessary and identify by block number)

The effects of cluster porosity on the tensile properties of T-1 steel butt-weldments were assessed in a program consisting of three phases of experimentation. In the first phase, cluster porosity was expressed as a percentage of the total cross section. In the second phase, cluster porosity was measured both in terms of the actual total area of pores and the area of the cluster (including metal ligaments, or webs, that connect pores). These two phases showed that the tensile strength of the welded metal is not

The contents of this report are not to be used for advertising, publication, or promotional purposes. Citation of trade names does not constitute an official indorsement or approval of the use of such commercial products. The findings of this report are not to be construed as an official Department of the Army position, unless so designated by other authorized documents.

DISCLAIMER NOTICE
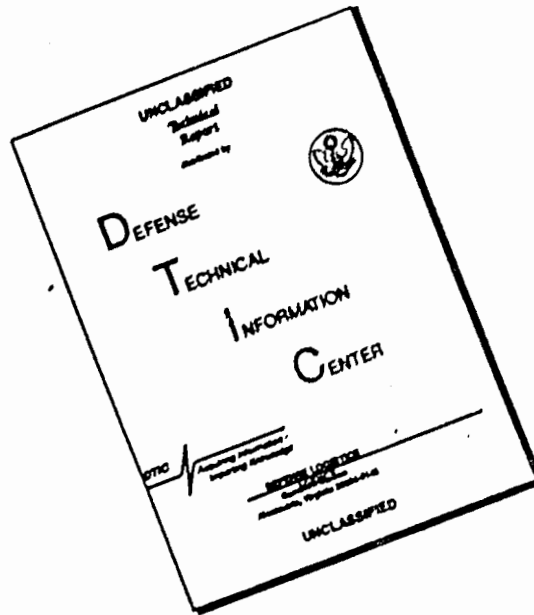
THIS DOCUMENT IS BEST QUALITY AVAILABLE. THE COPY FURNISHED TO DTIC CONTAINED A SIGNIFICANT NUMBER OF PAGES WHICH DO NOT REPRODUCE LEGIBLY.

significantly reduced if the area of pores and the cluster area are below critical sizes; however, ductility is rapidly reduced until these sizes are reached. The third phase established a partial correlation between cluster porosity size and the length of a center-crack in a plate. The J integral concept of fracture mechanics was used to examine the existence of a critical value of the J integral with which the critical pore area size (or other measure of cluster porosity) could be correlated. Consideration of the implications of this failure criterion on both working stress design and limit design indicate that relaxation of welding codes may be considered for certain applications if the codes are based on working stress design. Relaxation of codes based on limit design should not be considered for the conditions of porosity covered in this study.

FOREWORD

This investigation was performed for the Directorate of Military Construction, Office of the Chief of Engineers (OCE), under Project 4DM728012AOK1, "Engineering Criteria for Design and Construction"; Task 02, "Application Engineering"; Work Unit 102, "Engineering Criteria for Welds." The OCE Technical Monitor was I. A. Schwartz.

The investigation was performed by the Metallurgy Branch, Materials Systems and Science Division, U.S. Army Construction Engineering Research Laboratory (CERL). CERL personnel directly concerned with this study were K. W. Carlson and Dr. E. M. Honig Jr. Mr. Carlson was responsible for the design and execution of all experiments and for the analyses of data for most of the first and third phases of experimentation. Dr. Honig was responsible for the remainder of the data analyses, the conclusions obtained and the composition of this report.

Dr. R. Quattrone is Chief, Metallurgy Branch; I. J. Healy is Chief, Materials Systems and Science Division; COL M.D. Remus is Commander and Director of CERL, and Dr. L. R. Shaffer is Deputy Director.

CONTENTS

TABLES

FIGURES

FIGURES (cont'd)

6

EFFECTS OF CLUSTER POROSITY ON THE TENSILE PROPERTIES OF BUTT-WELDMENTS IN T-1 STEEL

1 INTRODUCTION

Problem. There is a need for acceptance guide specifications for welds based on actual mechanical behavior of a structural weld in any given application. To this end it is necessary to relate weld discontinuity characteristics—such as size, type, shape, location, orientation, and spacing—to mechanical properties of the weld. Such a relation is needed to replace the empirical approach currently used in most cases of specification for structural welds—an approach that often results in over- or under-designed welds.

This problem relates to military construction in that Engineer Field Offices are responsible for verifying the product quality in construction procurement. Accurate acceptance standards are required to assure confidence in the structural integrity of welded fabrications in the construction product.

Objective. Various types of weld defects (or discontinuities), such as cracks, porosity and inclusions, have been shown directly responsible for premature brittle facture of structural components. The purpose of this study was to evaluate the effect of cluster porosity on the tensile properties of T-1 steel weldments. Fracture mechanics relations, nondestructive tests, and static tensile tests were used to predict the dependence of these tensile properties on cluster porosity size.

This investigation provides a partial basis for the evaluation of inspection criteria relating allowable defect parameters to given levels of performance. These criteria would fulfill part of the needs stated above.

Historical Review. Pense and Stout[1] have recently reviewed the literature concerning the effects of porosity in welds. In that review it was noted that the earliest work performed by Baysinger and Rogerson concluded that scattered porosity had no effect on tensile strength until the porosity became "excessive." It was also noted that their study did not report data on the exact amount of porosity encountered. Later, according to the review, Mattek and Moodward attempted to correlate radiographic recordings of porosity in 410 stainless steel castings with the tensile properties of the castings. They concluded that the imperfections had little or no effect on the yield strength, so that porosity was not considered a limiting factor when designing on the basis of yield strength alone.

Green, Hamad, and McCauley[2] conducted studies of the effects of uniformly distributed porosity on the static and impact properties of a mild steel, AISI 1020. Porosity levels were measured from face and side radiographs and directly from the fracture surfaces. However, the actual method of measuring the porosity and the range in pore size were not reported. The results indicated that there was little decrease in the tensile strength until the porosity density reached about 7 percent. Specimens containing between 7 and 10 percent porosity exhibited considerable reduction and variation in strength. Thereafter, from 10 percent to the highest porosity level tested, the tensile strength did not decrease appreciably more. The measured average elongation decreased from an initial value of 20 percent in sound welds to approximately 18 percent at 7 percent porosity; beyond 10 percent porosity the effect was very large. The shape and distribution patterns of the porosity were found to have no noticeable effect on the tensile properties. It was not mentioned how the porosity was measured or what the sizes of the pores were.

Bradley and McCauley[3] investigated the effects of uniform porosity on a quenched and tempered steel, T-1. The porosity levels were measured from side and face radiographs and directly from the fracture surfaces. Static and impact tests were conducted with porosity levels up to 28 percent. It was found that little change in tensile strength occurred until the porosity approached 5 percent. Between 5 and 10 percent porosity there was some reduction in tensile

[1] A. W. Pense and R. D. Stout, "Influence of Weld Defects on the Mechanical Properties of Aluminum Alloy Weldments," Welding Research Council Bulletin No. 152 (July 1970), pp. ...

[2] W. L. Green, M. F. Hamad and R. B. McCauley, "The Effects of Porosity on Mild Steel Welds," The Welding Journal, Vol 37, No. 7, Research Supplement (1959), pp. 209s-306s.

[3] W. Bradley and R. B. McCauley, "The Effects of Porosity in Quenched and Tempered Steel," The Welding Journal, Vol 43, ... Research Supplement (1964), pp. 408s-414s.

strength and variability to the data; for amounts greater than 10 percent there was a more pronounced reduction in strength. The effect of porosity on elongation at fracture was found to be similar to its effect on strength—up to 5 percent porosity, the elongation was only slightly less than that for a sound weld; between 5 and 10 percent porosity, a large decrease was reported; and for amounts greater than 10 percent, the elongation at fracture decreased only slightly further. In general, it was concluded that the amount of porosity, rather than its shape, location, or distribution, most affected the strength and ductility properties of the T-1 steel weldments.

Lawrence, Radziminski, and Kruzic[4] reported that ultimate tensile strength in T-1 steel weldments was not appreciably affected until cluster porosity exceeded 4 percent. At 1 percent cluster porosity, the uniform strain in unflawed specimens was reduced from 20 percent to 9 percent. A method of multiple exposure radiography to determine flaw size was developed.

2 PROCEDURE

Program. The first phase of the test program consisted of studying 12 specimens containing clustered porosity. Numerous experimental problems, such as specimen warping during welding, were encountered. These problems, while not invalidating the data, did cast doubt on its reliability. In the second phase, which involved the study of six more specimens containing clustered porosity, the fabrication and testing conditions were more carefully controlled. Attempts to apply J integral analysis to the data of this phase suggested the need for J integral data from center-cracked specimens as a basis of comparison. The final phase of study consisted of testing five center-cracked specimens to determine how well clustered porosity could be modeled after a center-crack in a plate.

Materials. The base metal used was an ASTM A517 Type F structural steel, USS T-1. The weld wire was

Airco AX100. The chemical compositions of the base and filler metals are given in Table 1, and their mechanical properties in Table 2.

Fabrication. The tensile specimens were fabricated from 6 × 10 ft steel plate stock. The plates were flame cut into 10 × 36 in. blanks, and each of these was sawed in half. The sawed edges were machined to a double-vee 60° bevel as illustrated in Figure 1. Before welding, the beveled edges of the blanks were cleaned with acetone to insure oil- and dirt-free welding surfaces. A 100 F preheat was used to remove any moisture on the machined surfaces and thereby prevent the formation of linear porosity along the root pass.

All welding was performed using the gas metal-arc (GMA) welding process with an argon-2 percent oxygen shielding gas mixture; the welding parameters are listed in Table 3. The procedure consisted of the deposition of two weld passes, which completely filled one-half of the weld groove. The root pass was then back-ground using disc and carbide grinders, after which two additional passes were placed to complete the weld deposit.

The weldments containing internal defects were produced similarly to the sound welds except that the flow of the shielding gas was interrupted during the placement of the third pass.[5] This created an unstable arc, which in turn produced the clustered porosity. Interruption of the gas flow was accomplished using a solenoid-activated valve situated between the welding torch and the shielding gas tank; the shielding gas was reduced or turned off for varying lengths of time, depending upon the size of cluster desired.

After welding, the weld reinforcement was removed by disc grinding, and an initial radiograph was taken to determine the approximate nature and size of the porosity cluster produced. Using a template and shape-cutting unit, the welded blanks were then flame cut to the test specimen configuration shown in Figure 2. The flame-cut edges were filed and sanded in the direction of the longitudinal axis of the specimen. The specimen faces were then

[4] F. V. Lawrence, Jr., J. B. Radziminski, and R. W. Kruzic, *The Effect of Porosity on the Static Tensile Behavior of High Strength Structural Steel Weldments*, Technical Report UILU-ENG 73-2024 (University of Illinois, 1973).

[5] K. W. Carlson, F. V. Lawrence, Jr., and J. B. Radziminski, *The Introduction of Discontinuities in High Strength Steel Weldments*, Preliminary Report M-21 (Construction Engineering Research Laboratory [CERL], 1972).

milled flat and sanded to the same smoothness as the edges.

Each weldment was first examined by normal incidence radiography to determine the extent and location of weld defects. Stereoradiography, taken using the procedure of Carlson and Lawrence,[6] then provided greater understanding of the character of each defect.

The center-cracked panels were prepared from sound welds (soundness was determined by radiography). A starter notch in the plate center of the weld zone was drilled and cut according to ASTM recommended practice (Figure 3).[7] Fatigue cracks, using a tension-tension cycle of 5 to 115 ksi, were initiated in accord with ASTM Standard E399-70T. Growth of the fatigue cracks was monitored by a closed-circuit television camera with a rectangular grid superimposed for crack measurement. The observed external crack lengths $2a_e$ are given in Table 4. From 10 to 20 kilocycles at 4 Hz were required to propagate the cracks to the desired length.

Mechanical Testing. The specimens were mounted in a 600,000-pound capacity MTS tensile load frame and loaded directly to fracture at a constant rate of crosshead motion (.03 in./min). All tests were conducted at room temperature. The deformation occurring in a 1-inch gage length straddling the weld was measured with a linear variable differential transformer (LVDT) extensometer attached to the center-line of each specimen. The load and LVDT extension signals were recorded throughout the test with x-y plotters, and the load and LVDT signals were converted from analog DC to digital signals and recorded on magnetic tape. The latter step was performed to retain a separate permanent record of the data, especially if autographic plotting errors should later be discovered.

The percent strain was determined as the ratio times 100) of the measured extension to the gage length. The strain and stress at maximum load were termed the uniform strain, ϵ_u, and the ultimate

(tensile) stress, σ_u, respectively. The yield stress, σ_y, was determined at 0.2% plastic strain offset.

Fracture Surface Examination. After testing, the ends of the specimen halves were sawed off to permit easy measurement of the porosity clusters and storage of the fracture surfaces. Each fracture surface was examined to determine its nature and the actual dimensions of the cluster porosity defect. A photograph, roughly 2X, was made of each pair of fracture surfaces, as shown (somewhat reduced) in Figure 4a. The configuration of the fracture surfaces is even better understood when the thickness and face views are considered, as in Figures 4b and 4c, respectively.

In the first phase of the test program, the photograph of each specimen's fracture surface was overlaid with a grid and the porous area was determined by counting squares. The ratio (times 100) of this count to the total number of squares in the entire cross section was the percent porosity. In the second phase, both the area of the pores and the area of the region enclosing the pores on the fracture surface were determined by using a polar planimeter directly on the photograph. In the third phase, the fatigue-cracked area was determined by using a planimeter on the photograph of the fracture surface. The mean crack length 2a, cited in Table 4, was found by dividing the crack area by the specimen width.

Consider the projection of the fracture surface on the plane transverse to the tensile axis, as in Figure 4a. The *porous region intercepted by the fracture surface* is defined here as the least area, in this plane of projection, that contains all the projections of the pores visible on the fracture surface. In this region the greatest dimension parallel to the weld plane is defined as the *cluster length (fracture surface)*. The *cluster width* is the greatest dimension, in this region, transverse to the cluster length. Both the cluster width and length are transverse to the tensile axis.

Radiographic Evaluation. The weld quality of each specimen was evaluated by using the radiograph of the specimen and military specification MIL-R-11468(ORD), *Radiographic Inspection*. This is the controlling accept/reject document referenced in Corps welding guide specifications. Figure 4d shows a pre-fracture positive radiograph of specimen AS-21 in relation to photographs of the fracture

[6] K. W. Carlson and F. V. Lawrence, Jr., *The Examination of Discontinuities in Welds by Stereoradiography*, Technical Report M-24 (FRL, 1972)

[7] W. F. Brown, Jr. and J. E. Srawley, "Fracture Toughness Testing," *Fracture Toughness Testing and Its Applications*, ASTM STP 381 (American Society for Testing and Materials, 1965) p 191

surface that later passed through the specimen. The fracture surface is related further to the pre-fracture radiograph in the radiograph of the fracture surfaces of the ruptured specimen pieced together, as shown in Figure 4c.

The *porous region intercepted by a radiograph* is defined here as the least area that contains all the visible radiographic images of the pores. In this region, the greatest dimension parallel to the weld plane is defined as the *cluster length (radiographic)*. This dimension is parallel but not necessarily equal to the cluster length (fracture surface). This inequality follows from the fact that a cluster of porosities is three-dimensional, of unequal extent among the dimensions. Hence the projection of the cluster on the radiographic plane is not necessarily the same as the projection on any other plane. Moreover, through errors of radiographic technique, the radiographic images (or projections) of some pores may not be discerned.

3 RESULTS

First Phase. Table 5 gives results of cluster porosity tests for the first phase of the test program. Figure 5 shows the effect of porosity on the uniform strain, ϵ_u. The strain decreases from the sound weld value rapidly with increasing percent porosity—up to about 4 percent—and is much less sensitive to larger porosities. In Figure 6 the ultimate tensile strength, σ_u, displays a similar dependence on the cluster porosity—the rapid decrease in σ_u beginning at about 2 percent porosity. Figure 7 shows that the yield strength, σ_y, is not strongly affected by percent porosity and decreases only slightly as the percent porosity increases. Since these T-1 steel weldments did not have sharp yield points, these yield data are somewhat sensitive to the amount of plastic strain offset used in their computation.

Figure 8 shows the dependence of σ_u on the length of the porous region intercepted by the fracture surface, called the cluster length (fracture surface). When the cluster length is less than three times the cluster width, observed here to be less than ¾ in., this width influences σ_u heavily and produces some scatter in the curve. Above a cluster length (fracture surface) of about 1 in., the scatter in σ_u decreases rapidly as the cluster length increases. Similarly, Figure 9 shows the dependence of σ_u on the length of

the porous region as determined by a radiograph. This cluster length information, called cluster length (radiograph), is the information an inspector in the field would have available for most nondestructive weld examinations. This figure shows that σ_u decreases sharply with cluster length once a cluster length of about 1 in. is apparent on a radiograph. However, on a statistical basis, it is possible that Figures 8 and 9 have insufficient ranges of abscissas from which to draw these inferences.

The foregoing analysis indicates the qualitative nature of analyzing welds from radiographic images alone, since a single normal incidence radiograph cannot provide information on the depth (in the plate thickness direction) of a defect. This in turn emphasizes the qualitative nature of the accept/reject standards in MIL-R-11468 and in the welding codes of professional engineering societies.

Radiographic inspection of the specimens of this phase, in accordance with MIL-R-11468, showed that only specimen AS-7 could be accepted—and even then only as "borderline, standard III." This judgment was based on the observation that the porosities in this phase most nearly fitted the specification's "scattered cavities" classification. Specimen AS-7 was judged to be most comparable to radiographic standard C1-3 in the specification.

Second Phase. Table 6 gives results of the second phase of the test program. In this phase the independent experimental parameter is the area of the pores rather than percent porosity. Figure 10 shows the rapid decrease of uniform strain, ϵ_u, with pore area. Only about 0.03 in.^{2} pore area can be tolerated before ϵ_u is reduced to less than 5 percent. However, up to 0.20 in.^{2} pore area can be tolerated for which ϵ_u exceeds 3 percent. Similar results appear in Figure 11 for ϵ_u as a function of the area of the porous region. This region, the fracture surface projection defined in section 2, includes not only the pore area, but also the area of the connecting ligaments between the pores. If it is assumed that these ligaments rupture very early in the loading of the specimen, then the area of the cracked region at large loads would be this area enclosing the pores. A region about 0.09 in.^{2} causes ϵ_u to drop below 5 percent, yet up to 0.26 in.^{2} porous region can be tolerated for which ϵ_u exceeds 3 percent.

Figure 12 shows a nearly linear dependence of the

ultimate tensile strength, σ_u, on the area of the pores. However, the scatter in the dependence of the yield stress, σ_y, is broad, and no attempt has been made to pass a line or curve of correlation through those data. It is again clear that a pore area larger than about 0.03 in.^{2} causes a significant reduction in tensile properties, while such an area up to about 0.20 in.^{2} does not reduce σ_u below 110 ksi. In Figure 13, both σ_u and σ_y are fairly linearly related to the area of the porous region. These tensile properties decrease sharply when the pores are distributed over an area up to about 0.09 in.^{2}. However, over 110 ksi tensile strength can be maintained with a porous area up to 0.26 in.^{2}.

Figures 14 and 15 show fairly linear dependences of σ_u on the cluster length (fracture surface) and on the cluster length (radiographic). These figures are related to Figure 13 in that they pertain to the extent of the region having pores. The tensile properties are certainly affected for porous regions longer than about 0.4 in. or radiographic lengths larger than 0.6 in.

Radiographic inspection of the specimens of this phase in accordance with MIL-R-11468 showed that only specimens AS-23 and AS-26 could be accepted: AS-26 as "borderline, standard I" and AS-23 as "borderline, standard III." Using the classification "scattered cavities," as discussed earlier, specimen AS-26 was judged comparable to radiographic standard C1-2, while specimen AS-23 was judged comparable to standard C1-3. All other specimens in this phase were unacceptable.

Third Phase. Tensile data for the center-cracked specimens are presented in Table 7. Figure 16 shows that ϵ_u increases with increasing mean crack length. The strain here is determined from the displacement of the plate at its center-line. Since the plate can open more, axially, when the crack is longer, the positive slope of the curve in Figure 16 is understandable.

In Figure 17, the values of σ_u are tightly clustered about a stress of 92 ksi and a mean center-crack length of about 1 in., with the exception of one datum point. It appears that σ_u is not very sensitive to the length of center-crack in the specimens studied.

The energy required to obtain a given deflection

is shown in Figure 18 as a function of mean crack length. The larger the crack length, the less energy required to achieve a given deflection.

It is possible to calculate an effective mean crack length by adding a term to correct for the stress-relaxing effect of the plastically deformed zones at each crack tip. This term, called the *plastic zone radius*, can be determined from an elastic compliance relation,[8] or from such single terms as the strain energy release rate, G, or stress intensity factor, K.[9] The addition of this term to the mean crack length would shift all the abscissae of the center-crack data in Figures 16, 17, 18 and 21, and thus the curves in those figures, to slightly larger mean crack length values. But, since the plastic zone radius is not explicitly dependent on the deflection of the specimen, this curve shifting would not vary with deflection. Hence the relative positions of the center-crack data would remain unchanged. Consequently, the results of the foregoing discussion and the conclusions in the next section would not be altered by correcting crack-length data for plastic zone radii.

4 DISCUSSION

First and Second Phases. As Figures 6 and 7 indicate, up to about 2 percent porosity can be tolerated before the tensile properties become seriously affected. However, ductility is affected above 1 percent porosity, as shown in Figure 5. Ultimate tensile strength appears to be unaffected when the porous region is less than about 0.5 in. long (Figure 8), or has an effective radiographic length of less than 1 in. (Figure 9).

The quantitative effect of the pores can be measured in terms of their area. Figures 10 and 12 indicate that pore areas in excess of 0.03 in.^{2} cause a strong reduction in tensile strength, while ductility is markedly reduced at this defect size. The quantitative effect of pore *distribution* can be measured in

[8]R. J. Bucci, P. C. Paris, J. D. Landes, and J. R. Rice, "J Integral Estimation Procedures, *Fracture Toughness, Proceedings of the 1971 National Symposium on Fracture Mechanics Part II.* ASTM STP 514 (American Society for Testing and Materials, 1972), pp 40-69.

[9]W. F. Brown, Jr and J. E. Srawley, "Fracture Toughness Testing," *Fracture Toughness Testing and Its Applications.* ASTM STP 381 (American Society for Testing and Materials, 1965), pp 131-198.

terms of the area of the region occupied by the pores. Such an area up to about 0.09 in.[2] (Figure 13) causes a significant reduction in tensile strength, while Figure 11 shows that the same area range causes a sharp loss of ductility. The porous region area of 0.09 in.[2] seems to correspond to a cluster length (fracture surface) of about 0.4 in. (Figure 14), or an effective radiographic length of about 0.6 in. (Figure 15).

Application of Fracture Mechanics. In a recent study,[10] fracture mechanics was used to establish, in part, a critical size of weld defect below which tensile properties were unaffected. This was possible because (1) the fracture mechanics parameter used —the J integral—approached a constant value with increasing defect size, and (2) only one defect existed within each specimen tested.

A cluster of pores is not a single defect, however, but an aggregate of defects. A recent manuscript[11] showed that the metal (or continuum) bounding each pore contributes to the total value of the J integral as calculated from data pertaining to the entire specimen. Hence the total J integral will increase as the boundary of each pore is enlarged in the tensile test. The final value of the total J integral is determined, not by a limiting value characteristic of the material, but by the amount of deformation occurring at the time the boundary of one pore first reaches a critical J value and fracture ensues. Thus it would be futile in this report to search for a limiting value of the J integral for clusters of porosities, since such a limiting value cannot exist. To successfully apply the J integral at the current state of the art to cluster porosity, it would be necessary to obtain data for the boundary of, or for material influential on, each pore within the cluster. This is beyond the capabilities of current instrumentation.

Third Phase. The rationale behind the third phase of testing was to establish the center-cracked plate as a model of a cluster porosity in a plate. It was hoped that the mathematical treatment of the center-cracked plate in fracture mechanics could be applied successfully to cluster porosity.

To establish a correlation between the mechnical behavior of a cluster porosity and that of a center crack, one must relate the cluster size to the center-crack length. This relation may be established if one hypothesizes that, for each center-crack length, there is a single (or unique) cluster size that has the same deflection energy vs deflection relation as that center-crack length. In Figure 18, the deflection energies vs measured center-crack lengths at each of three deflections were plotted for the five center-cracked specimens from the third test phase, thus establishing the three curves shown. (At a fixed center-crack length, it is common for the deflection energy to increase with increasing deflection.)

In the same figure the deflection energy (at that deflection) of each of two specimens from phase one, and of six from phase two, was plotted on each of the three deflection curves. Since the deflection energy vs deflection relations of specimens AS-22 through AS-26 were essentially the same, they are represented by a single symbol. Moreover, specimens AS-4 and AS-1 ruptured before attaining the largest and second-largest, respectively, of the three deflections. Reference to the abscissa of the figure determines the center-crack length equivalent to each cluster size at that deflection.

From the figure, however, as the deflection changes, a given cluster size does not maintain constant equivalent center-crack size. Hence cluster size is not uniquely related to center-crack length—a contradiction of the above hypothesis. But, if a cluster could have a constant equivalent center-crack size, the load vs deflection curves of the two defects would have to be identical. This identity was not observed in this study; it is thus concluded that the center-cracked plate is not a complete, or perfect, model of a cluster porosity for fracture mechanics purposes.

Despite the failure of the center-cracked plate as a general model for cluster porosity, it is possible to derive some J integral information from the center-cracked specimens themselves. In the study by Lawrence and Cox[12] it is shown that, at any given deflection, δ, the J integral, J(δ), is given as an

[1] F. V. Lawrence, Jr. and F. P. Cox, *The Effect of Lack of Penetration Defects on the Static Tensile Behavior of High Strength Structural Steel Weldments*, Technical Report (Draft) (CERL, 1974).

[11] E. M. Honig, Jr., *Multiple Connectivity and the J Integral of Fracture Mechanics*, Technical Manuscript M-85 (CERL, 1974).

[12] F. V. Lawrence, Jr. and F. P. Cox, *The Effect of Lack of Penetration Defects on the Static Tensile Behavior of High Strength Structural Steel Weldments*, Technical Report (Draft) (CERL, 1974).

energy per net cross-sectional area by

$$J(\delta) = \frac{[2E(\delta) - P(\delta)\delta]}{Bb} \qquad [Eq\ 1]$$

where

$E(\delta)$ = total deflection energy at δ,
$P(\delta)$ = load at δ,
B = specimen thickness,
b = sum of ligaments in plane of crack.

The deflection energy $E(\delta)$ can be determined by mechanically integrating with a polar planimeter over the load-deflection curve to the deflection δ. Values of $J(\delta)$ are plotted against δ in Figure 19. Calculations of J were terminated at deflections at which the specimens were judged to be in a state of plane stress. The calculated values apply to a presumed state of plane strain. The trend is for smaller crack sizes (shown in parentheses beside their curves) to require larger J values to obtain the same deflection. The close grouping of four of the curves suggests a low sensitivity of the J integral to crack size in that range of crack sizes.

Lawrence and Cox found that a nearly linear correlation exists between the J integral value at maximum load, $J_M = J(\delta_{max})$, and the product $\sigma_{net\ max}\,\delta_{max}$. Here δ_{max} is the deflection at maximum load and $\sigma_{net\ max}$ is the stress, based on the net cross section, at maximum load. Similar computations were performed in the present study and are presented in Figure 20. Here a nearly linear relation exists for $J_M > G_{IcBM}$, the crack-opening (I) mode linear elastic energy release rate per unit crack extension for a free-running crack in the base metal. The one datum point not obeying this linear relation still lies quite close to $G_{IcBM} = 1.1$ ksi-in. (estimated from U.S. Steel data [13]). This supports the assertion of Lawrence and Cox that J_M has a lower limiting (or average) value and that such a value for the weld metal lies close to the critical G_I in the base metal. However, the strength of this corroboration is reduced by examining Figure 21. There are two crack sizes near 1 inch for which $J_M \gg G_{IcBM}$. Crack lengths both above and below 1 inch have J_M values near G_{IcBM}. This con-

flicts with the assertion of Lawrence and Cox that J_M rises far above G_{IcBM} only when the crack size is too small for valid J measurements. In the present case, the conflict could be resolved if the effective critical crack sizes of specimens CC-1 and CC-4 were far larger, possibly on the order of 2 in. Moreover, comparison of these fatigue-induced crack data to the lack-of-penetration data of Lawrence and Cox may not be justified. The two anomalously high values of J_M have not been reconciled.

Effect of Experimental Results and Construction Design Criteria on Weld Specifications.

Broadly speaking, there are two construction design philosophies, or criteria, commonly in use. The older criterion is "working stress design," in which only elastic strains are permitted in the structure. This design criterion is thus quite conservative, since only very small deflections are permitted. The new criterion is "limit design" in which (not accounting for factors of safety) the structure is allowed to be loaded to the yield point as long as a large amount of ductility can be obtained. Consequently, this design criterion is far less conservative than the older one. Although these criteria are actually not nearly as simple as stated, these statements do show the rough distinctions between the two design philosophies.

Welding codes do not explicitly state which of the above criteria are reflected in weld specifications. The AWS *Structural Welding Code* D 1.1-72, in discussing the permissible weld design stresses of new buildings and bridges, states that "the permissible stresses . . . for complete joint penetration groove welds . . . shall be those allowed for the same kind of stress for the base metal" and that "the base metal stresses shall be those specified in the applicable Building Code"[14] such as the codes of AISC and AASHTO. The AISC code, section 1.5.1.1,[15] states that the allowable tensile stresses in structural steel may be as large as $0.6\ \sigma_{ym}$ (except at pin holes) but not greater than $0.5\ \sigma_{um}$, where σ_{ym} and σ_{um} are the minimum values of the yield and ultimate strengths, respectively, for the grade of steel of interest. The AISC commentary on the code states that the basic working stress factor of safety is 5/3

[13] S. T. Rolfe and S. R. Novak, *Slow-Bend K_{Ic} Testing of Medium Strength High Toughness Steels*, Technical Report 49.018.007(1) of U. S. Steel Corp. 1969).

[14] *AWS Structural Welding Code*, AWS D1.1-72 (American Welding Society, 1972), pp 80, 86.

[15] *Specification for the Design, Fabrication, and Erection of Structural Steel for Buildings* (American Institute of Steel Construction, 1969), pp 5-16.

with respect to σ_{ym} and that, at the net section of axially loaded members, the factor of safety is 2 with respect to σ_{um}.[16] The AASHTO code for bridges states that the design stress for axial tension in members without holes is 0.55 σ_{ym}.[17]

From the *Steel Design Manual*, σ_{ym} = 100 ksi and σ_{um} = 115 ksi for T-1 A514 Grade F steel in the size tested in this program.[18] For the AISC code, the safety factor must be 2 and the design stress 57.5 ksi. For the AASHTO code, the design stress must be 55 ksi. If these codes were applied to the data of phase two, the respective design stresses would drop only by about 5 ksi—to 54 ksi and 50 ksi, respectively. This suggests that, for welding codes based on working stress design, cluster porosity in the extent studied here may not significantly degrade the quality of weldments under axial tension. Thus, in these cases, relaxation of cluster porosity restrictions in welding codes may be considered.

This concept is supported by the results of the weld quality evaluation performed in this study in accordance with MIL-R-11468. This specification condemns all but three of the welds in this study— yet Figure 6 shows ten welds having ultimate strengths in excess of 120 ksi, and Figures 12 and 13 show five welds with ultimate strengths exceeding 110 ksi. It is quite plausible that these 15 welds would have sufficed for a static tensile load in a working stress design. Rejection of these welds for such an application probably would accomplish nothing but increased project costs. Less stringent radiographic standards might thus be beneficial.

However, as Figures 5, 10 and 11 show, a marked reduction in ductility of weldments occurs when even small amounts of porosity are introduced. This implies that relaxation of welding codes based on limit design concepts would be undesirable, since the ductility required in that design is lost in porous weldments. One example of such a limit design application is found in Section III of the ASME

Boiler and Pressure Vessel Code.[19] In this code, the algebraic difference between the largest and smallest principal stresses is defined as the stress intensity, S. For a given material, the largest S permitted is denoted S_m, and is usually $\sigma_{um}/3$. In the code requirements for Class I components operating under normal and upset conditions, some combined loading cases allow a peak stress intensity of 3 S_m, which is essentially the yield strength value. It is evident that no reduction in ductility or tensile strength could be tolerated in such a critical design.

Strict application of radiographic specification MIL-R-11468 in this study eliminated all but the most ductile welds. Such rejection would be essential to the proper implementation of a limit design. Thus, a reduction in the quality of radiographic standards would not be beneficial in a limit design.

5 SUMMARY

Conclusions

1. There is a combination of pore size (in terms of total area of pores) and distribution of porosity (in terms of area encompassed by pores, i.e., the area of the porous region) that is critical in the sense that the tensile strength is not degraded until that pore size or porosity distribution is surpassed. In this study the critical pore area is about 0.03 in. and the critical area of the porous region is about 0.09 in.^{2}.

2. There is a similar combination of pore size and distribution of porosity that is critical in that the ductility (as measured by ϵ_u) is sharply degraded until that pore size or porosity distribution is surpassed; beyond the critical point the rate of degradation is reduced. In this study the critical pore area is about 0.03 in. and the critical area of the porous region is about 0.09 in.^{2}.

3. There is a critical radiographic length of cluster porosity associated with the critical combinations in Conclusions 1 and 2. In this study, the tensile strength was unaffected for radiographic lengths less than 0.6 in., while the ductility dropped sharply until that length was reached.

"Commentary on the Specification for the Design, Fabrication, and Erection of Structural Steel for Buildings (American Institute of Steel Construction, 1969), pp 5-122.

"Standard Specifications for Highway Bridges, 11th ed. (American Association of State Highway and Transportation Officials, 1973), p 112.

"Steel Design Manual (United States Steel, 1968), p 32.

"Nuclear Power Components," ASME Boiler and Pressure Vessel Code, Section III, Subsections NA and NB (American Society of Mechanical Engineers, 1974).

4. A critical size, or other measure, of cluster porosity cannot be predicted by the J integral of fracture mechanics at the current state-of-the-art.

5. Cluster porosity size, either in terms of area of pores or of area of the porous region, can be correlated with center-crack length on a deflection-energy basis, but a given cluster cannot be said to have a unique equivalent center-crack length.

6. In view of the relation of tensile strength to critical cluster porosity size, relaxation of weld inspection specifications may be possible for certain applications if the specification is based on working stress structural design criteria. However, considering the marked reduction in ductility with increasing porosity, relaxation of weld specifications based on limit design criteria should not be considered.

Future Work. The AWS, AISC, and AASHTO codes contain specifications for the *shear* of weldments that are distinct from those for the *tension* of weldments. Data on the shear of weldments containing cluster porosity should be acquired to determine the extent of degradation of the yield and ultimate shear stresses and uniform shear strain. This will test the question of whether working stress design may be unnecessarily conservative in shear as well as in tension of weldments.

Table 1

Chemical Composition of Base Metal and Welding Electrode

Manufacturer	Base Metal*	Welding Electrode**
	U.S. Steel Corporation	Air Reduction Co., Inc.
Designation	T-1	Airco AX110
Plate Thickness	3/4 in.	—
Electrode Type	.	1/16 in. bare wire

Element	Chemical Composition, %	
C	.15	0.084
Mn	.89	1.54
P	.009	0.008
S	.027	0.008
Si	.27	0.45
Ni	.80	2.43
Cr	.52	0.049
Mo	.42	0.48
V	.06	0.008
Al	—	0.004
Ti	—	0.0075
Zr	—	0.004
B	.0015	—
Cu	.21	—

*Data from independent analysis

**Data supplied by manufacturer

Table 2

Tensile Properties of Base Metal and Weld

Properties	Base Metal*	Weld**
Tensile Strength, ksi	120.8	140.0
Yield Strength, ksi	113.1	126.3
Elongation at Fracture, %	36.0 in 2.0 in.	50+ in ¾ in.
Reduction in Area, %	66.4	---

*Properties of base metal provided by manufacturer

**Average of three specimens taken from weld metal (from F. V. Lawrence, Jr. and
E. P. Cox, *The Effect of Lack of Penetration Defects on the Static Tensile Behavior
of High Strength Structural Steel Weldments*, Technical Report (Draft) (CERL,
1974).

Table 3

Welding Parameters

Voltage, V	Current, amps	Travel Speed, in./min	Interpass and Preheat Temp. F	Heat Input, kJ/in.	Shielding Gas Comp.
22-24	340-360	11	200	44	98 Ar 2 O₂

Table 4

Crack Lengths of Center-Cracked Specimens

Designation	Mean Length 2a (in.)	External Length, 2a_e (in.)
CC-1	0.88	0.74
CC-2	1.08	0.94
CC-3	1.07	0.45
CC-4	0.77	0.70
CC-5	1.36	1.24

Table 5

Results of Cluster Porosity Tests, First Phase

Specimen Number	Porosity (%)	Ultimate Tensile Strength σ_u (ksi)	Yield Stress, σ_y (ksi) (0.2% offset)	Uniform Strain, ε_u (%)	Reduction in Area (%)	Cluster Length (Radiographic) (in.)	Cluster Width** (Radiographic) (in.)	Cluster Length (Fracture Surface) (in.)	Cluster Width (Fracture Surface) (in.)
S-1	0	130.4	122.5	5.63	14.2	0	0	0	0
CN-2	0	133.8	123.2	>3.75*	*	0	0	0	0
AS-1	10.39	119.4	119.4	0.61	3.4	1.33	0.38	1.38	0.32
AS-2	9.79	120.9	120.9	0.45	2.8	1.40	0.40	1.30	0.36
AS-4	3.08	130.7	125.1	1.52	4.4	1.19	0.33	0.80	0.26
AS-5	3.94	122.0	122.0	0.53	4.2	1.42	0.36	1.16	0.20
AS-6	3.20	124.3	120.1	1.48	5.1	1.03	0.31	0.92	0.20
AS-7	1.15	131.1	123.7	1.84	4.5	0.91	0.33	0.50	0.20
AS-8	4.06	123.9	122.6	0.73	4.2	1.02	0.32	0.86	0.30
AS-9	3.76	122.2	118.1	1.26	4.5	0.98	0.37	0.60	0.30
AS-10	5.83	122.3	121.2	0.79	3.4	1.16	0.33	0.96	0.30
AS-11	4.70	125.7	122.4	0.93	3.5	1.17	0.43	1.68	0.24
AS-12	5.58	122.3	121.7	0.51	3.3	1.07	0.34	1.08	0.30

*Extensometer capacity exceeded by extension at maximum load
**This is greatest dimension perpendicular to cluster length (radiographic) in the radiographic plane.

Table 6

Results of Cluster Porosity Tests, Second Phase

Specimen Number	Area of Pores (in.²)	Ultimate Tensile Strength σ_u (ksi)	Yield Stress, σ_y (ksi) (0.2% offset)	Uniform Strain, ε_u (%)	Reduction in Area (%)	Cluster Width** (Radiographic) (in.)	Cluster Length (Radiographic) (in.)	Cluster Length (Fracture Surface) (in.)	Cluster Width (Fracture Surface) (in.)
AS-21	0.264	107.8	94.3	2.03	4.02	0.40	1.33	1.29	0.31
AS-22	0.194	111.1	98.6	3.81	4.51	0.43	1.10	0.84	0.31
AS-23	0.124	114.6	91.1	3.53	4.02	*	0.60	0.41	0.22
AS-24	0.122	111.1	92.9	3.49	11.87	0.41	1.00	0.92	0.27
AS-25	0.137	113.6	95.3	4.27	1.02	0.40	0.75	0.77	0.31
AS-26	0.030	117.1	97.1	4.80	1.28	0.38	0.70	0.63	0.22

*Linear porosity (split cluster)
**This is greatest dimension perpendicular to cluster length (radiographic) in the radiographic plane.

Table 7

Results of Center-Cracked Plate Tests

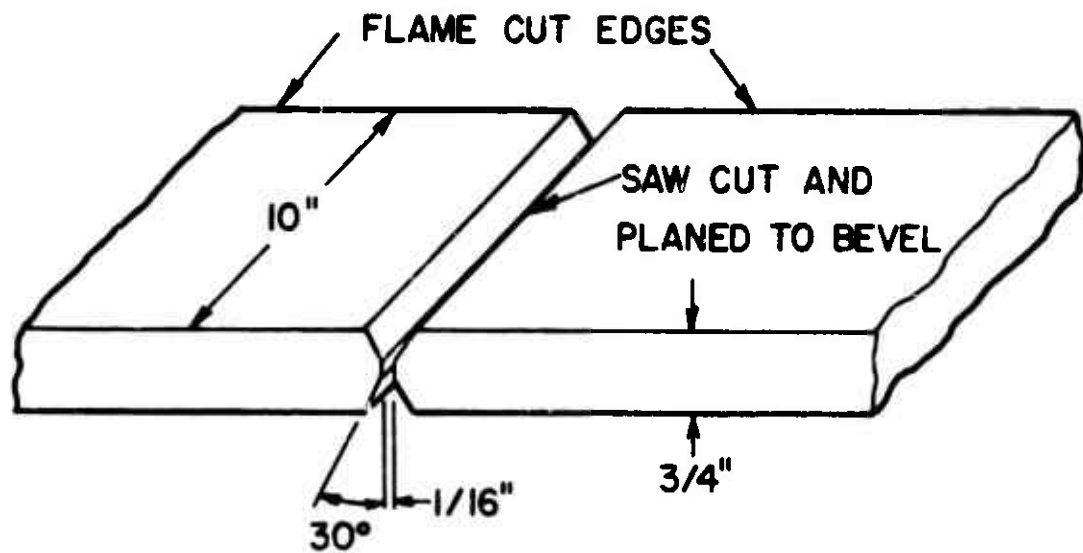| Specimen Number	Ultimate Tensile Strength, σ_u (ksi)	Uniform Strain, ε_u (%)	Reduction in Area (%)
CC-1	92.5	1.83	8.72
CC-2	94.4	3.64	9.19
CC-3	91.3	2.73	12.95
CC-4	90.0	1.27	8.72
CC-5	72.4	2.18	12.03

17

Figure 1. Edge preparation.

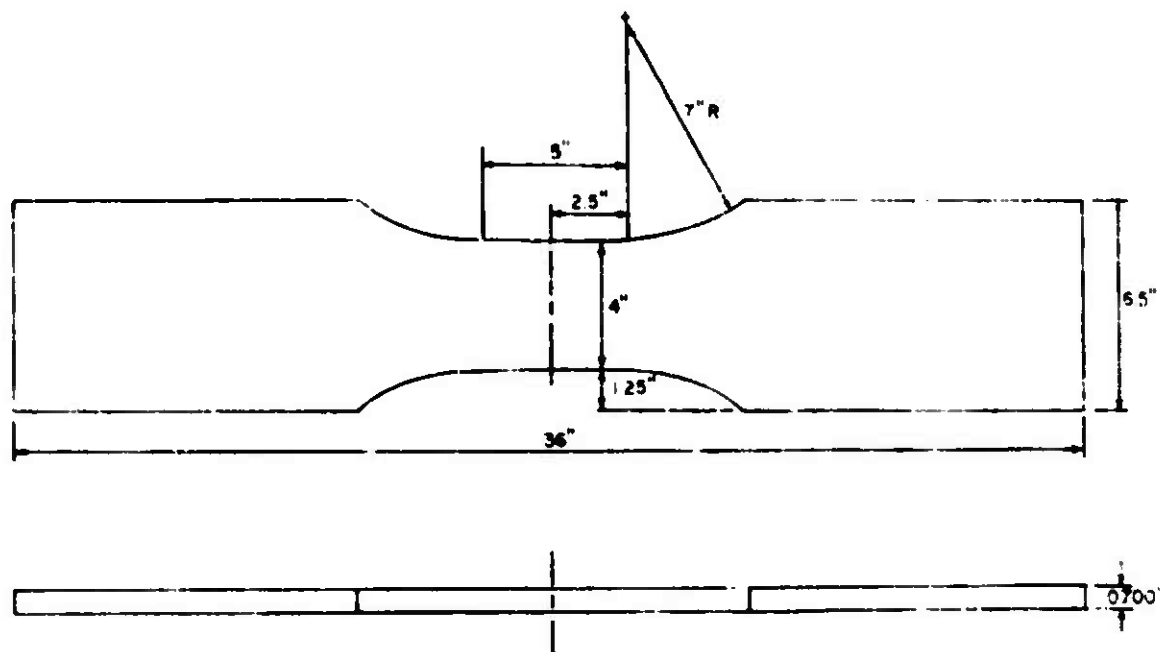**Figure 2.** Tensile specimen.

18
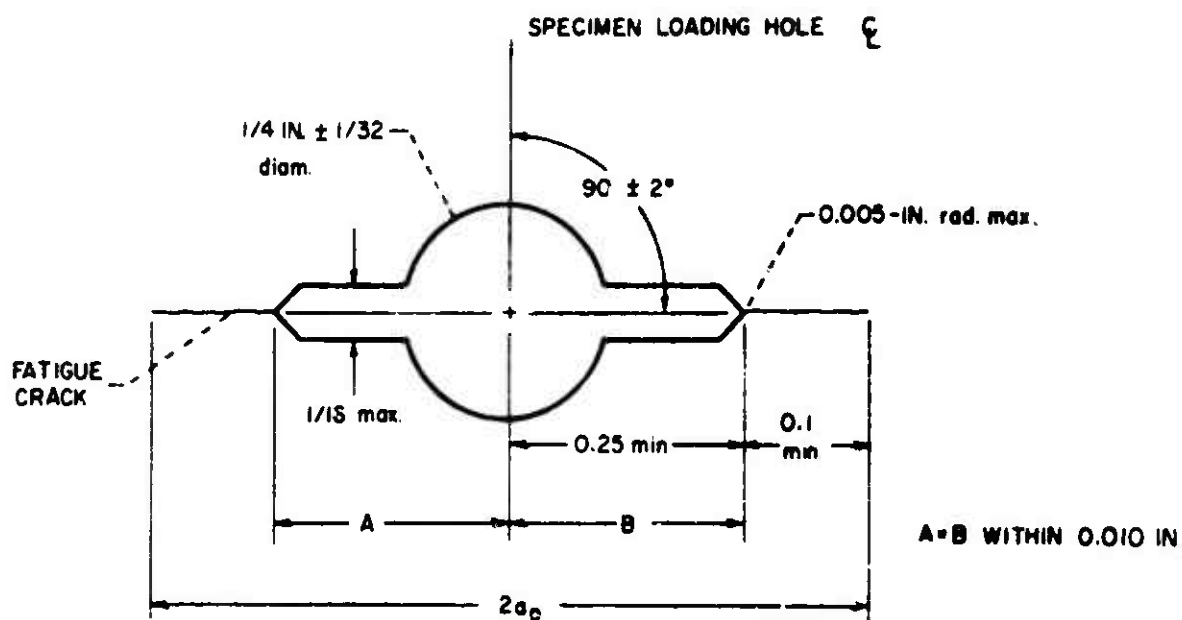
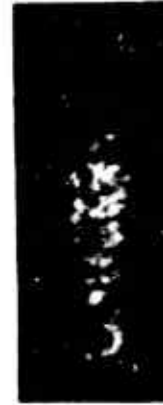**Figure 3.** Fatigue crack starter for center-crack plate specimens.

14

b. thickness view (2X)

a. tensile axis view (0.82X)

d. radiographic projection of (c) before fracture

e. radiographic projection of (c) after fracture

c. face view (0.76X)

Figure 4. Typical fracture surface passing through a clustered porosity.

20
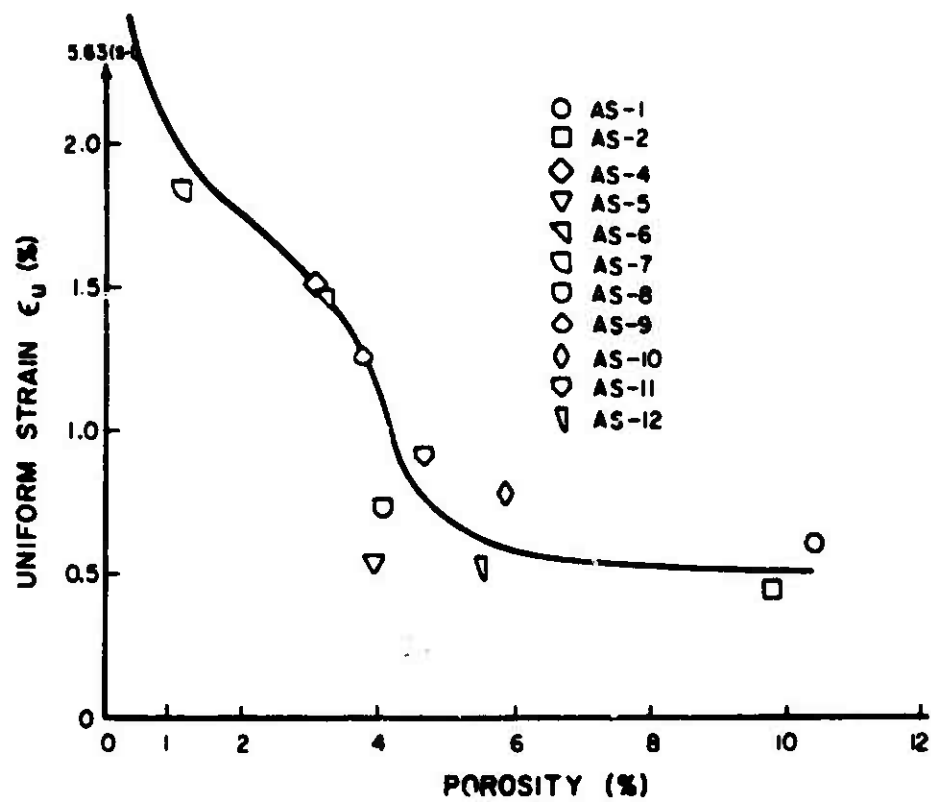
Figure 5. Uniform strain vs porosity.
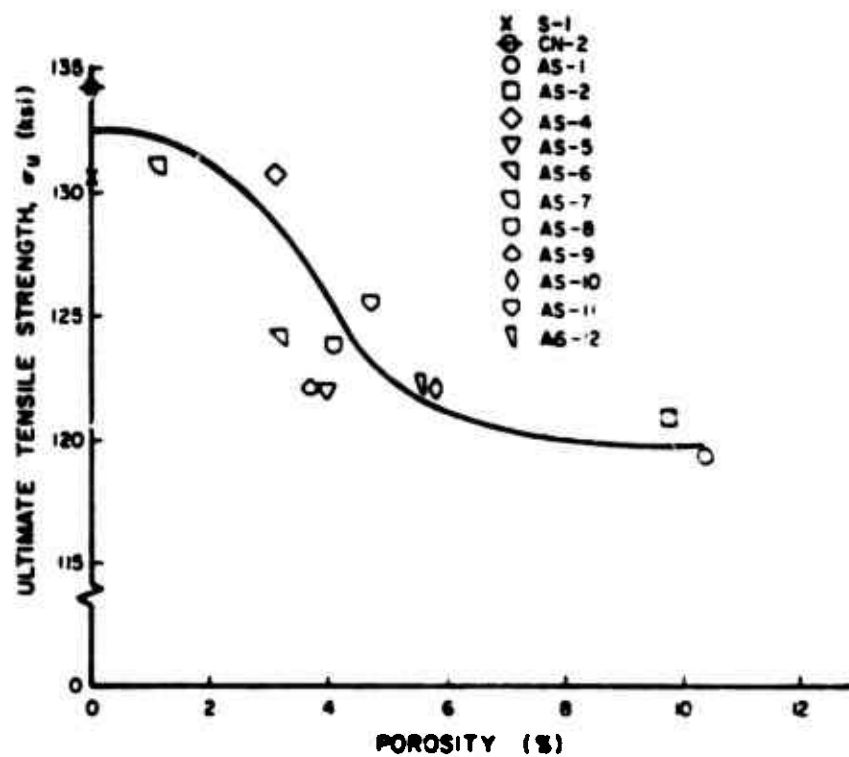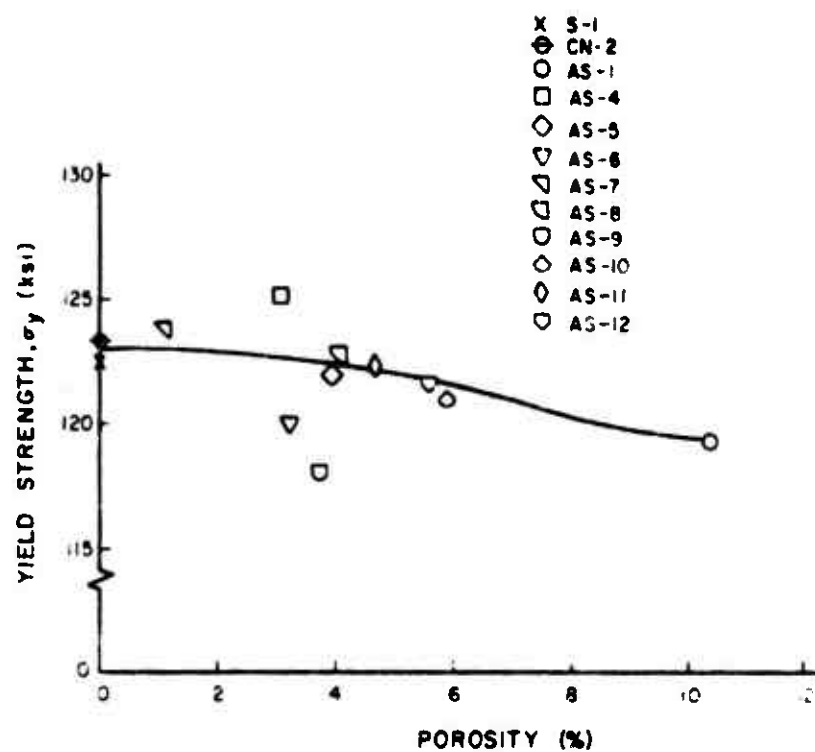

Figure 6. Ultimate tensile strength vs porosity.

21

Figure 7. Yield strength vs porosity.
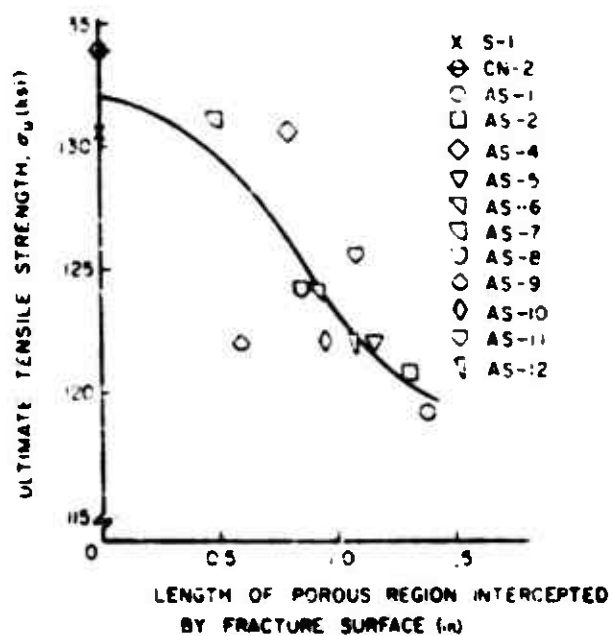
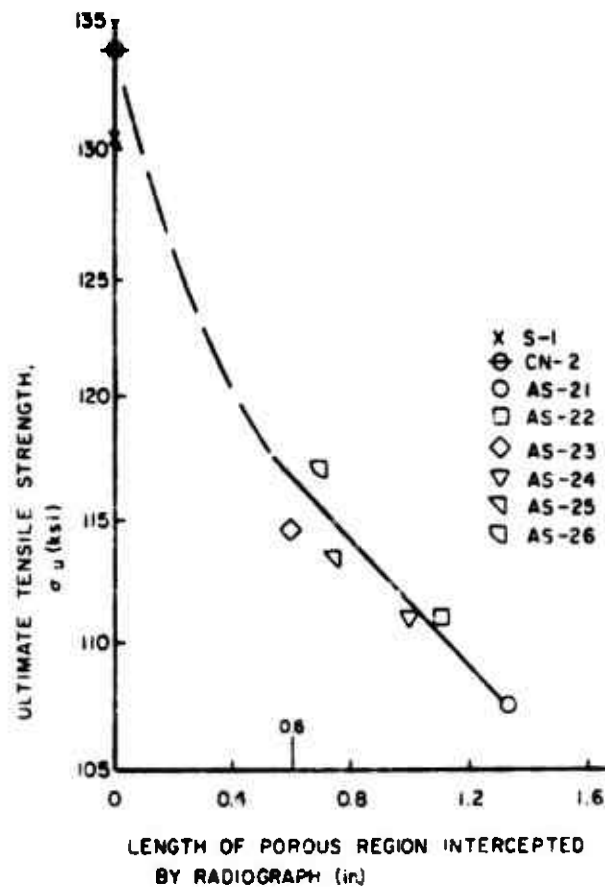**Figure 8.** Ultimate tensile strength vs length of porous region intercepted by fracture surface.

22
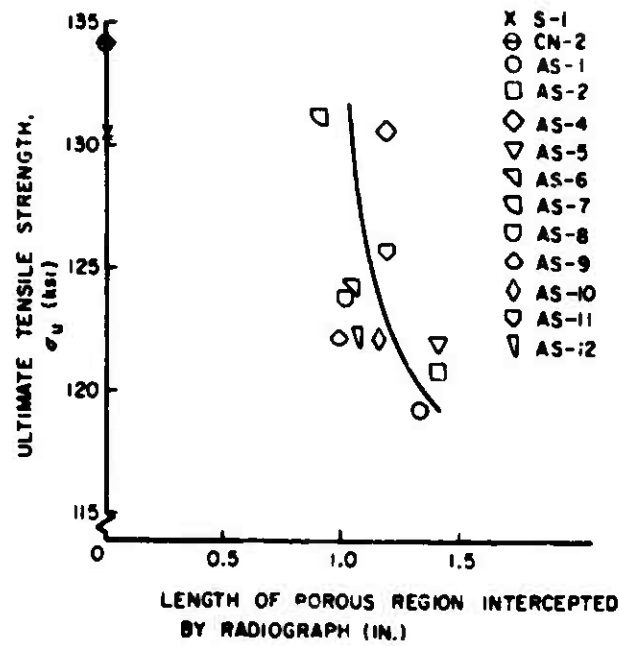
Figure 9. Ultimate tensile strength vs length of porous region intercepted by radiograph.
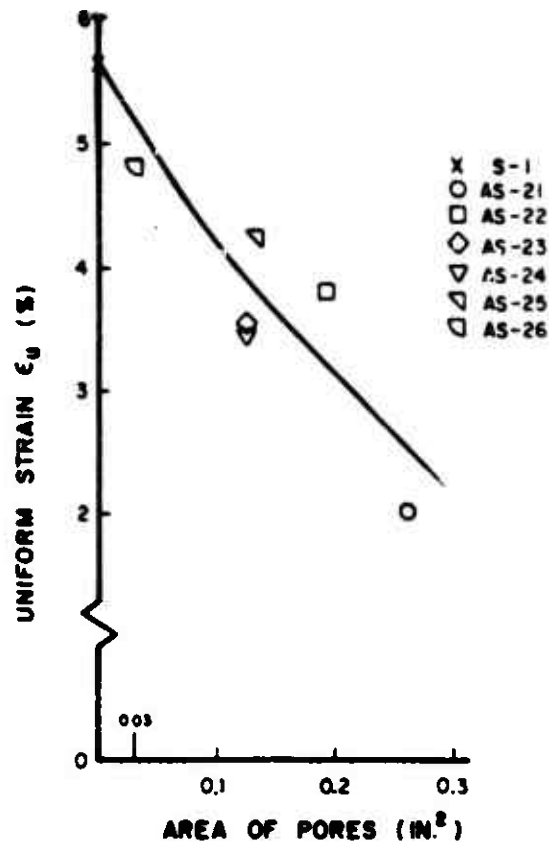

Figure 10. Uniform strain vs area of pores.

23
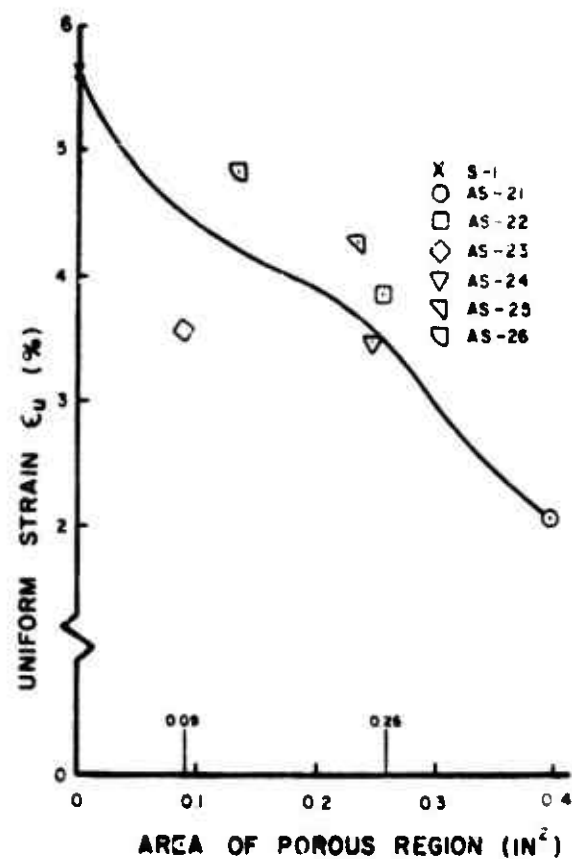
Figure 11. Uniform strain vs area of porous region.
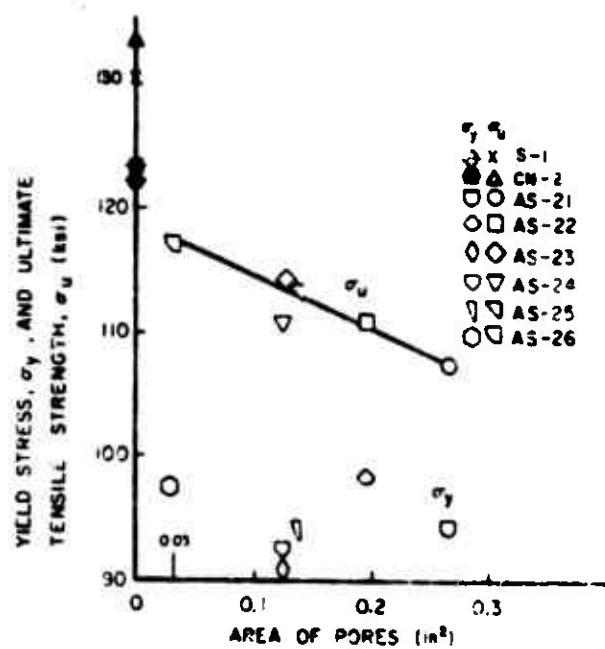
Figure 12. Yield stress and ultimate tensile strength vs area of pores.
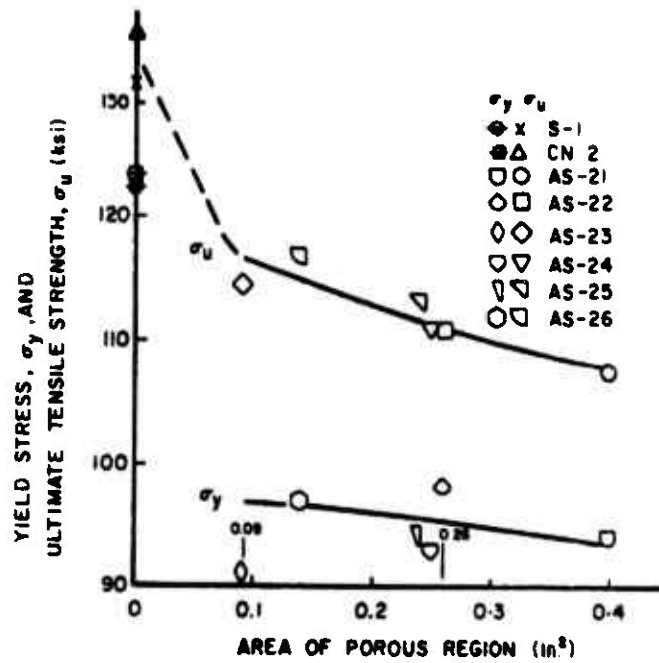
Figure 13. Yield stress and ultimate tensile strength vs area of porous region.
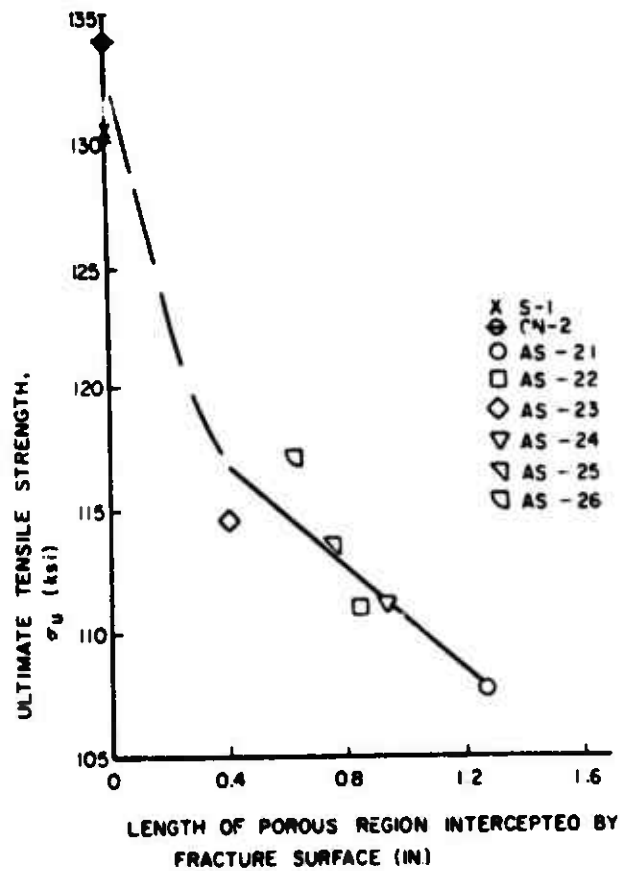
Figure 14. Ultimate tensile strength vs length of porous region intercepted by fracture surface.

Figure 15. Ultimate tensile strength vs length of porous region intercepted by radiograph.
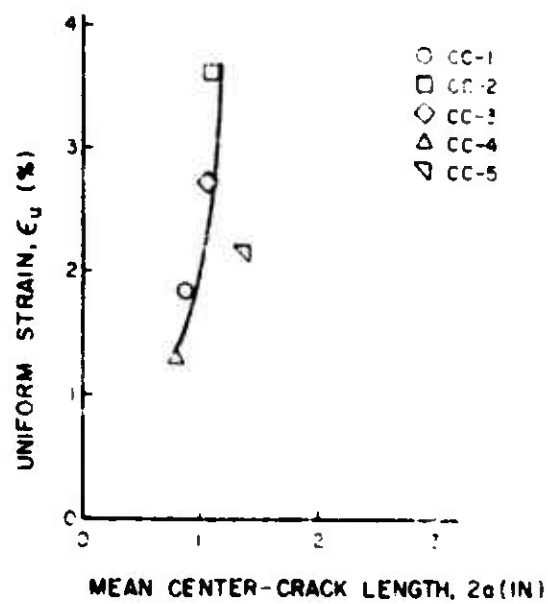
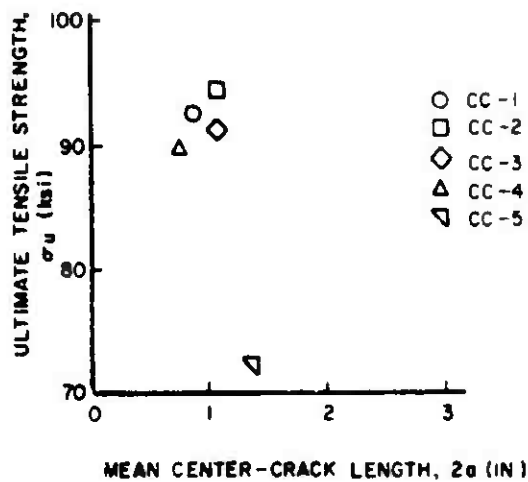**Figure 16.** Uniform strain vs mean center-crack length

Figure 17. Ultimate tensile strength vs mean center-crack length.
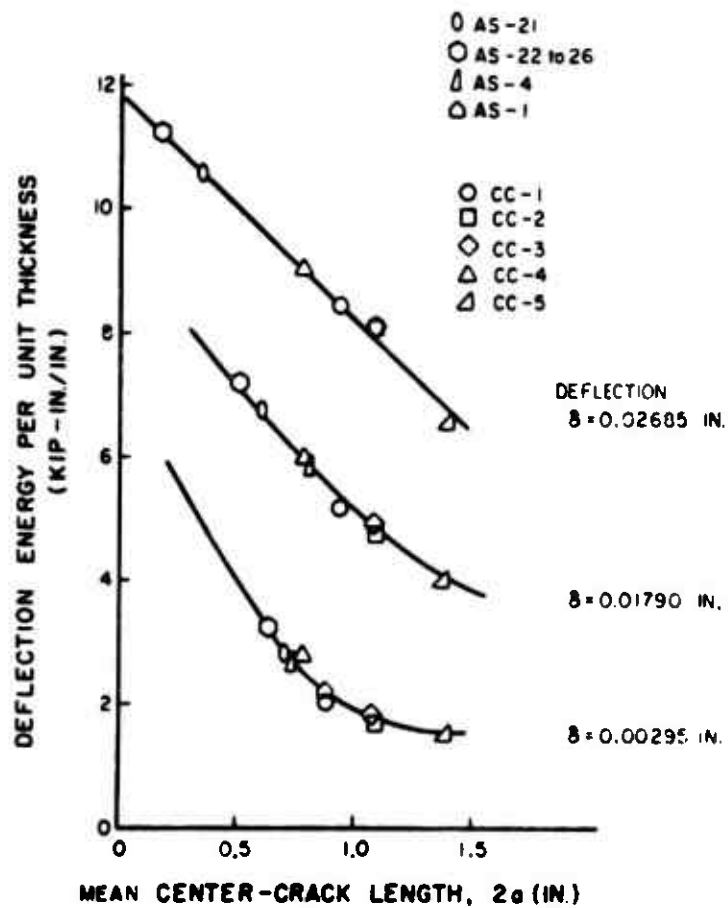

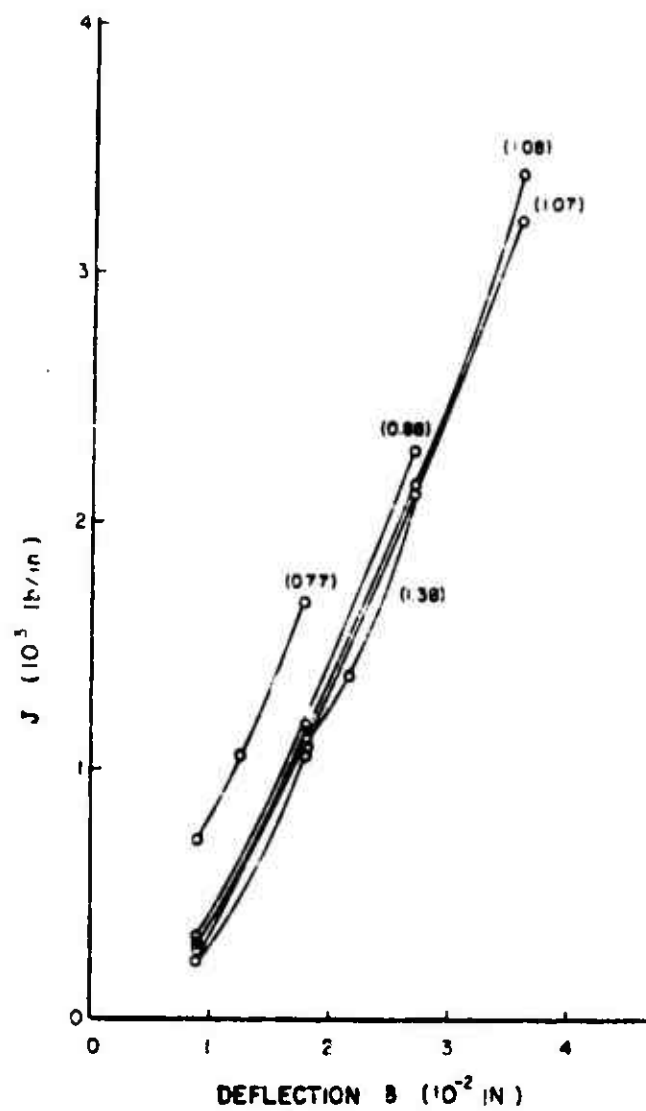**Figure 18.** Deflection energy per unit thickness vs mean center-crack length.

27

Figure 19. J vs deflection (center-crack lengths appear in parentheses beside their curves).
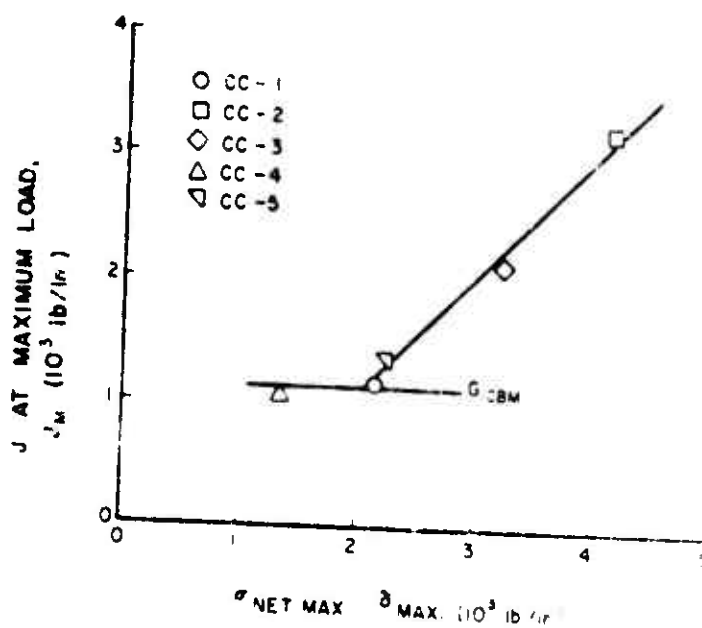
28

Figure 20. J at maximum load vs $\sigma_{net\ max}\ \delta_{max}$.
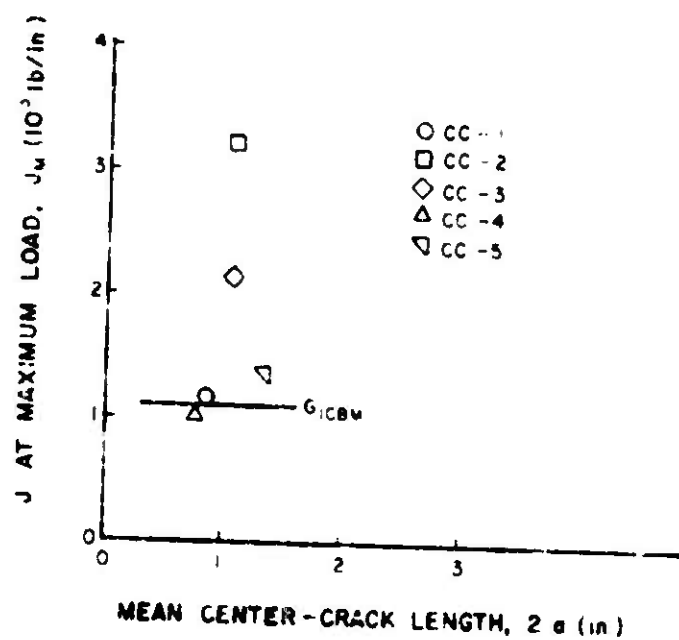

Figure 21. J at maximum load vs mean center crack length

REFERENCES

AWS Structural Welding Code. AWS D1.1-72 (American Welding Society, 1972), pp 80), 86.

Bradley, J. W. and R. B. McCauley, "The Effects of Porosity in Quenced and Tempered Steel," *The Welding Journal*. Vol 43, No. 9, Research Supplement (1964), pp 408s-414s.

Brown, W. F., Jr. and J. E. Srawley, "Fracture Toughness Testing," *Fracture Toughness Testing and Its Applications*. ASTM STP 381 (American Society for Testing and Materials, 1965), pp 133-198.

Bucci, R. J., P. C. Paris, J. D. Lande and J. R. Rice, "J Integral Estimation Procedures," *Fracture Toughness, Proceedings of the 1971 National Symposium on Fracture Mechanics. Part II*. ASTM STP 514 (American Society for Testing and Materials, 1972), pp 40-69.

Carlson, K. W. and F. V. Lawrence, Jr., *The Examination of Discontinuities in Welds by Stereoradiography*. Technical Report M-24 (Construction Engineering Research Laboratory [CERL], 1972).

Carlson, K. W., F. V. Lawrence, Jr., and J. B. Radziminski, *The Introduction of Discontinuities in High Strength Steel Weldments*. Preliminary Report M-27 (CERL, 1972).

Commentary on the Specification for the Design, Fabrication, and Erection of Structural Steel for Buildings (American Institute of Steel Construction, 1969), pp 5-122.

Green, W. L., M. F. Hamad, and R. B. McCauley, "The Effects of Porosity on Mild Steel Welds," *The Welding Journal*. Vol 37, No. 7, Research Supplement (1959), pp 209s-306s.

Honig, E. M., Jr., *Multiple Connectivity and the J Integral of Fracture Mechanics*. Technical Manuscript M-85 (CERL, 1974).

Lawrence, F. V., Jr. and E. P. Cox, *The Effect of Lack of Penetration Defects on the Static Tensile Behavior of High-Strength Structural Steel Weldments*. Technical Report [draft] (CERL, 1974).

Lawrence, F. V., Jr., J. B. Radziminski, and R. W. Kruzic, *The Effect of Porosity on the Static Tensile Behavior of High-Strength Structural Steel Weldments*. Technical Report UILU-ENG-71-2024 (University of Illinois, 1971).

"Nuclear Power Components," *ASME Boiler and Pressure Vessel Code*. Section III, Subsections NA and NB (American Society of Mechanical Engineers, 1974).

Pense, A. W. and R. D. Stout, "Influence of Weld Defects on the Mechanical Properties of Aluminum Alloy Weldments," *Welding Research Council Bulletin* (July 1970), pp 1-16.

Rolfe, S. T. and S. R. Novak, *Slow-Bend K_{Ic} Testing of Medium Strength, High-Toughness Steels*. Technical Report 39.018-007(11) (U.S. Steel Corp, 1967).

Specification for the Design, Fabrication, and Erection of Structural Steel Buildings (American Institute of Steel Construction, 1969), pp 5-16.

Standard Specifications for Highway Bridges. 11th ed. (American Association of State Highway and Transportation Officials, 1973), p 112.

Steel Design Manual (United States Steel, 1968), p 32.